Novel Imaging Systems: Multivariate Optical Computing in the UV-VIS

Ryan J. Priore, Ashley E. Greer, Frederick G. Haibach
Maria V. Schiza, David L. Perkins, and Michael L. Myrick
Department of Chemistry and Biochemistry, University of South Carolina
Columbia, South Carolina

Abstract

Imaging Multivariate Optical Computing (MOC) is a powerful analytical tool that combines digital imaging and predictive spectroscopy without the use of a spectrometer. Traditional techniques for multivariate analysis are both time consuming and costly involving expensive multi-channel instruments, difficult computations on large data sets and confinement to the laboratory. By encoding an angle-tolerant spectral pattern specific to a target analyte onto an interference filter, a snapshot of the chemical distribution and concentration can be obtained quickly and inexpensively.

This paper summarizes the advances in chemical imaging utilizing angle-tolerant Imaging Multivariate Optical Elements (IMOE) from the UV to visible regions of the spectrum using uncollimated sources. Two applications are demonstrated using both transmission and diffuse reflectance data. These optical elements are fabricated via reactive magnetron sputtering of alternating layers of high and low refractive index materials, (Nb_2O_5 and SiO_2, respectively). A single CCD camera in a swivel design rotating about the IMOE filter axis is employed for both transmittance and reflectance imaging. Our current UV diffuse reflectance technique miniaturizes the chemical imaging prototype with a catadioptric image-splitting prism block and a single monochrome camera controlled by a handheld computer.

Introduction

Chemical or hyperspectral imaging is a rapidly developing field with both microscopic and macroscopic applications ranging from materials characterization to remote environmental sensing. Hyperspectral imaging has matured in the last two decades and is now routine with the advent of multichannel array detectors and tunable wavelength filters but still suffers from long data collection times and the need for post computer processing using multivariate analyses.[1] Significant challenges remain in obtaining reasonable spectral and spatial resolution, signal-to-noise ratio (SNR), sample preparation, speed and cost.

Multivariate optical computing (MOC) attempts to combine the data collection and processing steps in a traditional multivariate chemical analysis in a single step. It offers an all-optical computing technology with no moving parts.[2] The system is also inexpensive to manufacture in a compact, field-portable design. Its speed due to an all-optical calculation can offer real-time measurements with relatively high SNR.

Traditional multivariate techniques like Principle Component Regression (PCR) and Partial Least Squares (PLS) extract spectral patterns related to pure component spectral variations and analyte concentrations. A regression or loading vector may be calculated from a training set of mixture spectra to correlate analyte concentration with the magnitude of the spectral pattern. Our laboratory produces encoded spectral vectors called Multivariate Optical Elements (MOE) via reactive magnetron sputtering to perform chemical measurements. MOEs are designed such that the difference between their transmittance and reflectance are proportional to the regression vector. They may be fabricated with only a few layers using an optimization algorithm to minimize the analyte prediction error.[3]

MOEs are designed to perform with collimated light in a beam-splitter configuration at 45º for point detection measurements. A further application for MOEs is in chemical imaging by separating sample spectral information into separate channels of a red-green-blue (RGB) image. Unlike MOEs, Imaging Multivariate Optical Elements (IMOE) perform with a small angular distribution of non-collimated incident light around 45º (Figure 1) while still maintaining the ability to perform a reliable chemical measurement.

Light passing through the MOE-based optical system produces an analog signal proportional to the chemical property of interest.[4] The optical computation to be performed is thus the scalar product of the loading vector with the sample spectrum given by:

$$\hat{y}_i = \sum_{j=1}^{N} I(\lambda_j) x_i(\lambda_j) \qquad (1)$$

where $l(\lambda_j)$ is the loading vector at wavelength j, $x_i(\lambda_j)$ is the spectral intensity of the sample at wavelength j, $\hat{y}_i$ is the scalar product result and j is the index running over all N wavelengths of the spectrum. The transmission and reflection spectrum of the MOE can be denoted as:

$$T(\lambda_j) = 0.5 + l(\lambda_j) \tag{2}$$

$$R(\lambda_j) = 0.5 - l(\lambda_j) \tag{3}$$

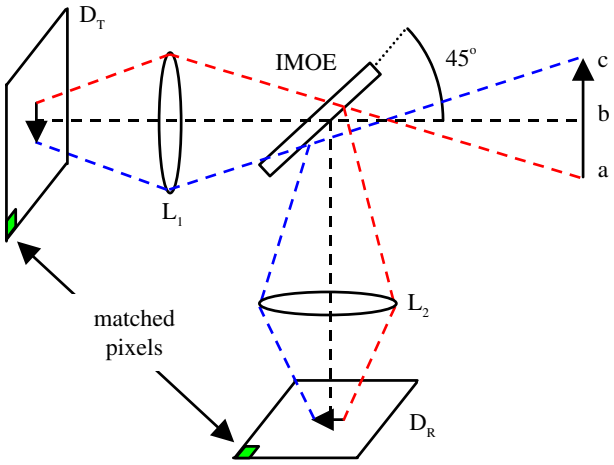

Figure 1. IMOE arranged in a beam-splitter configuration. D_T and D_R are the transmitted and reflected light detector. L_1 and L_2 are focusing lenses. a, b and c represent the minimum, mean and maximum angles of incident light on the IMOE.

For a non-absorbing filter, the MOE transmits 50% of the incident light plus the loading vector at each wavelength, while the MOE also reflects 50% minus the loading vector at each wavelength. Subtracting $R(\lambda_j)$ from $T(\lambda_j)$ and substituting into Equation 1 for $l(\lambda_j)$ results in:

$$\hat{y}_i = \frac{1}{2}\sum_{j=1}^{N}\left[T(\lambda_j) - R(\lambda_j)\right]x_i(\lambda_j) \tag{4}$$

A gain (G) and offset (off) are introduced to adjust the proportional measurement, $\hat{y}_i$ to equal the analyte concentration prediction. This also defines the MOC Regression Vector (R_v).

$$\hat{y}_i = \frac{1}{2}\sum_{j=1}^{N} G\left[T(\lambda_j) - R(\lambda_j)\right]x_i(\lambda_j) + off$$
$$\hat{y}_i = \sum_{j=1}^{N} R_v(\lambda_j)x_i(\lambda_j) + off \tag{5}$$

The shape of $l(\lambda)$ can be found by minimizing the error in predicting a set of spectra where the chemical concentration is known. The mean square difference between the known sample concentrations and that predicted is known as the standard error of prediction (SEP). The SEP relates the error in analyte concentration prediction to the true analyte concentrations from the validation data set and is the figure of merit for designing a MOE.

$$SEP = \sqrt{\frac{\sum_{i=1}^{N}(y_i - \hat{y}_i)}{N}} \tag{6}$$

Our laboratory has already demonstrated the prediction of a target analyte concentration as a point-detection scheme in the presence of a single interfering chemical species without the need of post computer processing using an MOE.[5] This report details the first demonstration of MOC using an IMOE as well as two instrumental designs, a swivel and miniature prototype for MOC chemical imaging with a single camera. Simple binary mixtures of Bismarck Brown (BB) and Crystal Violet (CV) were used to design an IMOE for BB detection. *Bacillus globigii* spore solutions were utilized on a paper background to design a simple bandpass interference filter for spore detection. The experiments reported consist of both MOE and instrumental prototype design and fabrication results.

Experimental

A. Swivel Prototype

The transmission MOC imaging instrument was constructed from Linos Photonics (Milford, MA) optical components. The optical train pivoted about the MOE axis to use a single camera for both transmittance and reflectance images with respect to the MOE (Figure 2). Three plates of PVC were placed in front of the source lamp to diffuse the incoming radiation ensuring that multiple angles of incidence existed on the MOE over the visible spectrum from 400-650 nm.

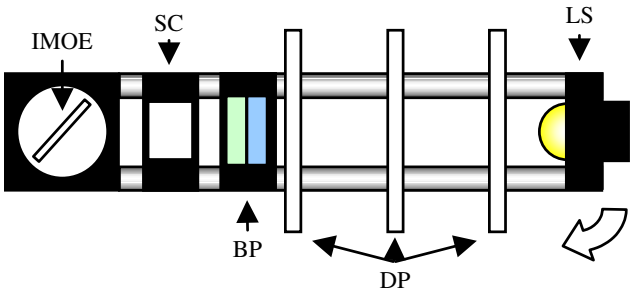

Figure 2. Swivel Imaging MOC Instrument. IMOE is the interference filter, SC is the sample cell, BP is the bandpass filters, DP is the diffuser plates and LS is the tungsten light source.

An ST-6 CCD (Santa Barbara Instrument Group, Santa Barbara, CA) was radiometrically calibrated using an OL Series 750D grating double-monochromator (Optronic Laboratories, Inc., Orlando, FL). The source package consisted of two Schott glass filters (Duryea, PA), BG-39 and GG-400, to isolate the visible spectral region, a 6-V/6-W tungsten filament lamp (Linos Photonics) with a 1 × 1.2-mm active filament and diffuser plates. This source package was calibrated against an OL Series 455 integrating sphere calibration standard lamp (Optronic Laboratories, Inc.) using the same system used to calibrate the CCD.

Stock solutions of BB (λ_{max} = 457 nm, dye content 50%) and CV (λ_{max} = 590 nm, ACS reagent grade, dye content 50%) in distilled water were prepared at concentrations of 416.16 μM and 125.01 μM respectively. Fifty mixtures of BB and CV were prepared by dilution following a 5^2 full-factorial experimental design with three additional midpoint mixtures used as long-term repeats. The concentrations of the dye mixtures varied such that the minimum transmittance in the 400-650 nm spectral range was 30-70%. BB was selected as the analyte with CV as an uncorrelated interference at all wavelengths over which BB absorbed. A Perkin Elmer UV-visible spectrometer (model Lambda 14, Wellesley, MA) was used to record optical spectra of the mixtures in a 1-cm fused-silica cell (Starna Cells Inc., Atascadero, CA).

The radiometric data was convoluted with the optical spectra to produce system response curves from which an angle-tolerant IMOE was designed.[6] The IMOE was fabricated by a custom-built reactive magnetron sputtering (RMS) system (Corona Vacuum Coaters, Vancouver, BC) by alternating 14 layers of Nb_2O_5 and SiO_2 onto a 1-mm thick BK-7 glass substrate.

The deposition process was monitored online via grating monochromator (Scientec Inc., London, Ontario, Canada) and a photomultiplier tube (model H5784-03, Hamamatsu, Japan) from 420-640 nm. Each layer was monitored at a single wavelength to monitor deposition. A complete spectrum was taken to determine the thickness of each completed layer before an online reoptimization of the filter design was performed to correct for deposition inaccuracy.[7] An in-house LabView 6.0 "virtual instrument" operating in conjunction with the Corona Vacuum Coaters system control software governed this monitoring and deposition process.

A validation set of binary solutions was created following a 5^2 full-factorial experimental design for the imaging experiment. Transmission and reflection images were collected in the rotating prototype for each sample. The CCD integrated for 9 seconds at a high resolution of 375×241 pixels.

B. Miniature Prototype

The diffuse reflectance MOC imaging instrument was fabricated in house. Four ½-inch prisms (Edmund Industrial Optics, Barrington) and an aluminum coated glass slide (Fischer Scientific, Pittsburgh, PA) were used to form the stereo imaging block enabling a single camera to collect both transmittance and reflectance images simultaneously (Figure 3).

A monochrome camera (model WAT-660A, Watec America Corp., Las Vegas, NV) and blue and yellow light emitting diodes (LEDs) (λ_{max} = 430 nm and λ_{max} = 595 nm, Gilway, Woburn, MA) were radiometrically calibrated as the detector and source using the aforementioned procedure. Diffuse reflectance data were acquired of *bacillus globigii* on paper envelope media for qualitative analysis. A bandpass filter was fabricated after visual inspection of the calibration and diffuse reflectance data to separate the reflected light where the envelope and *bacillus globigii* possess the highest spectral variation (around 400 nm). The 23-layer bandpass filter was fabricated using power and time estimates by RMS onto a single prism. The block was then masked to reduce stray light and cemented together with lens bond (type DB=99, Summers Optical, Fort Washington, PA). A drop of *bacillus globigii* solution (concentration = 26.09×10^7 spores/mL) was placed on a paper envelope and imaged with the miniature prototype.

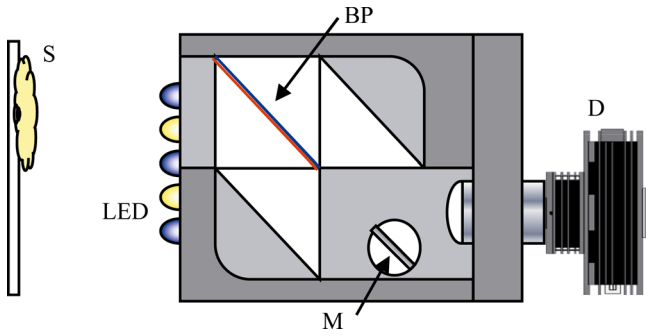

Figure 3. Catadioptric Imaging Mini-MOC Instrument. BP is the bandpass filter, S is the sample on paper, M is the mirror, D is the miniature monochrome camera and LED is the set of LEDs.

Results & Discussion

A. Swivel Prototype

The spectral profile of an interference filter undergoes a blue shift when the filter is tilted away from normal incidence. A non-imaging MOE performs ideally at 45º where the encoded vector is most orthogonal to the interfering species vector. Its predictive ability drastically decreases at angles other than 45º since the encoded regression vector shifts along with the transmission profile. IMOEs are angle-tolerant whereby the regression vector retains its predictive ability over a small range of incident angles around 45º.

The experimentally determined regression vector differed from the calculated vector in the red portion of the visible spectrum (Figure 4). This was at a fault of the online monitoring system that measures the filter deposition at normal incidence. The mismatched region truly occurred at wavelengths outside of our deposition system's ability to monitor and control. The problem presents itself when the

filter is tilted away from normal incidence; the calculated and measured SEPs differ by more than a factor of two.

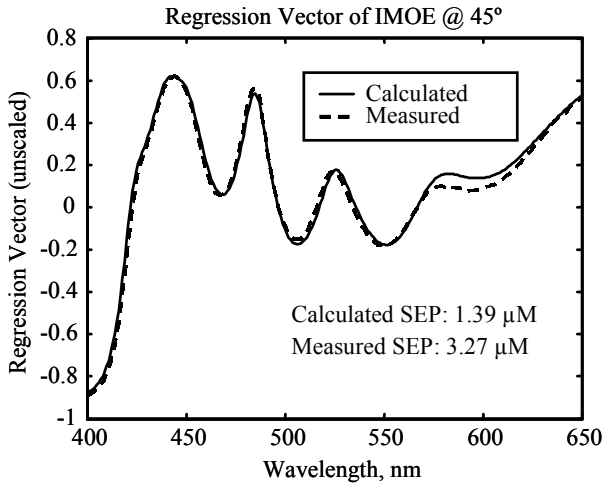

Figure 4. Comparison between the final calculated and the experimentally determined regression vector.

A partial correction was introduced by scaling intensity values in the reflection image since the optical train alignment differs slightly from the transmission image. Using the correlation coefficient (R^2) as the optimization parameter, difference images were collected with reflection balances from 0.8-1.2 and averaged portions of the image set were fit using a linear regression. The optimal balance was chosen to be 1.122 where the R^2 was maximized. The gain, offset and SEP were determined experimentally from a 30×30 averaged pixel area in the center of the each image using the linear regression model after applying this balance to the recalculated image set (Figure 5).

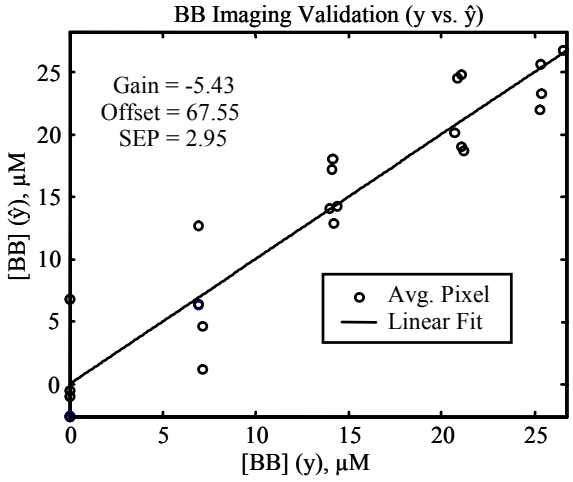

Figure 5. Averaged pixel intensities used to determine the system gain, offset and SEP by linear regression.

RGB composite images were created by subtracting the magnitude of the difference image from the green and blue channels while leaving the red channel blank (Figure 6).

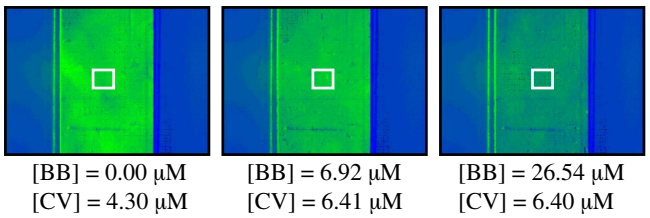

Figure 6. RGB composite MOC images of binary mixtures in a quartz cell correlated with BB concentration. The white boxes display the area averaged to determine the system gain, offset and SEP.

B. Miniature Prototype

The transmission and reflection *bacillus globigii* drop images were extracted from the raw image using an in-house LabView 6.0 "virtual instrument" to detect stain boundaries and perform the image subtraction. A difference image was constructed from the extractions, and a gain of 4 utilized to increase the image contrast. An RGB image was created where the green channel contained the difference of the extractions, the blue channel contained the sum of the extractions and the red channel was left blank (Figure 7).

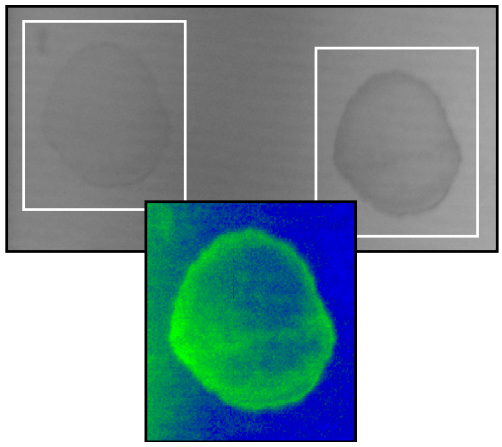

Figure 7. RGB composite images of bacillus globigii drop on envelope paper media.

Unlike the swivel prototype, the image-splitting mini-prototype was specifically designed for utilizing a single camera without moving the optical train. A single, fixed camera eliminates an experimental gain adjustment between two identical detectors synonymous with our current MOE-based MOC approach. The detector balance was evaded with this prototype, although the images formed at the

detector were parallax inducing stereo images as seen in the resulting difference image (Figure 7). A proper image-splitting single-camera prototype should ensure identical optical path lengths for both images to eliminate unequal focal points and background intensity gradients.

Conclusions

We have demonstrated two chemical imaging applications in the UV-VIS based on MOE-based MOC technology. These prototypes based on interference filters offer a portable, low cost alternative to chemical imaging in both transmission and diffuse reflectance applications. Without the need for post multivariate analysis and specialized scientific instrumentation, chemical imaging could potentially extend to everyday applications performed by the layman.

Acknowledgements

Effort sponsored by the Human Effectiveness Directorate, Air Force Research Laboratory, Air Force Materiel Command, USAF, under grant number F33615-00-2-6059. The U.S. Government is authorized to reproduce and distribute reprints for Governmental purposes notwithstanding any copyright notation thereon. The views and conclusions contained herein are those of the authors and should not be interpreted as necessarily representing the official policies or endorsements, either expressed or implied, of the AFRL Human Effectiveness Directorate or the U.S. Government.

The authors would like to acknowledge Arthur Illingworth for the fabrication of the miniature prototype.

References

1. Paul Geladi and Hans Grahn, *Multivariate Image Analysis*, John Wiley & Sons, Chichester, 1996.
2. Michael Myrick, Olusola Soyemi, Jeevananda Karunamuni, DeLyle Eastwood, Hong Li, Lisa Zhang, Ashley Greer and Paul Gemperline, *Vib. Spectrosc.*, **28**, 73 (2002).
3. Olusola Soyemi, Frederick Haibach, Paul Gemperline and Michael Myrick, *Appl. Spectrosc.*, **56**, 477 (2002).
4. Matthew Nelson, Jeff Aust, George Dobrowolski, Pierre Verly and Michael Myrick, *Anal. Chem.*, **70**, 73 (1998).
5. Olusola Soyemi, DeLyle Eastwood, Lisa Zhang, Hong Li, Jeevananda Karunamuni, Paul Gemperline, Ron Synowicki and Michael Myrick, *Anal. Chem.*, **73**, 1069 (2001).
6. Olusola Soyemi, Frederick Haibach, Paul Gemperline and Michael Myrick, *Appl. Optics*, **41**, 1936 (2002).
7. Frederick Haibach, Ashley Greer, Maria Schiza, Ryan Priore, Olusola Soyemi and Michael Myrick, *Appl. Optics*, **42**, 1833 (2003).

Biography

Ryan J. Priore is in the third year of a Ph.D. program in Analytical Chemistry at the University of South Carolina. He received a B.S. in Chemistry from the University of Pittsburgh. In 2000 he completed an internship with ChemImage Corp. working on a Raman chemical imaging microscope. He is currently developing novel hyperspectral imaging techniques using interference filters to perform optical computations under the supervision of Michael L. Myrick. He is a member of the Society for Applied Spectroscopy.